VOLUME - 15, ISSUE - 04, APRIL - 2026 • PRINT ISSN No. 2277 - 8160 • DOI : 10.36106/gjra

Original Research Paper

Engineering

PUMPED TWO-PHASE R2L DIRECT-TO-CHIP COOLING IN HIGH-DENSITY DATA CENTER RACKS: SYSTEM DESIGN AND EXPERIMENTAL EVALUATION

Utkarsh Dagor Sr. R&D Mechanical Engineer, Anoka, MN, USA

ABSTRACT Data centers are experiencing rapidly escalating thermal loads driven by AI/HPC workloads with chip TDPs now exceeding 1–2 kW. This study presents the design and testing of a pumped two-phase, direct-to-chip refrigerant-to-liquid (R2L) cooling system for high-density racks. The test setup features an in-row R2L coolant distribution unit (CDU) rated at 160 kW (scalable toward 180–200 kW) integrated with row- and rack-level manifolds feeding server cooling loops, each loop containing four micro-channel cold plates. Thermal Test Vehicles (TTVs) with 2.5 kW cartridge heaters (2,500 mm² area) emulated up to 10 kW per server. The system was evaluated under varied hydraulic conditions and heat loads, focusing on pressure drops in supply manifolds, loop regulators, and returns. Two-phase heat transfer to chilled water (using R-134a) was highly effective: at ~0.50 LPM/kW, the maximum CPU case temperature (T_case) was ~55–56 °C, well below typical 80 °C reliability limits. Pressure drops remained modest (≈0.23 psi across row manifolds, up to ~7.6 psi in rack loops at full load). These results confirm that two-phase R2L cooling can safely dissipate >160 kW per rack at high efficiency and suggest that even higher-capacity systems (e.g., 200 kW CDUs in production) are viable. The use of low-GWP refrigerants (e.g., R-515B, GWP 299) is recommended for future systems to improve sustainability. Overall, pumped two-phase direct-to-chip cooling emerges as a promising, energy-efficient solution for next-generation high-density data centers.

KEYWORDS : Two-phase Cooling; Direct-to-chip; Refrigerant-to-liquid (R2L); Data Center Thermal Management; Microchannel Cold Plates; R-134a; R-515B; CDU; AI/HPC; Energy Efficiency

1. INTRODUCTION

Modern data centers face unprecedented thermal challenges. AI accelerators and GPUs now have thermal design powers on the order of 1–2 kW per device, and rack-level densities often exceed tens of kilowatts per rack. Traditional air-cooling is no longer adequate—25–40% of a data center's energy can be consumed by the cooling system itself. Pumped two-phase liquid cooling (P2P) leverages the latent heat of vaporization to capture heat at the chip package and transport it with minimal temperature rise. In two-phase direct-to-chip (D2C) systems, a refrigerant is circulated through cold plates in thermal contact with processors: it boils on the chip, absorbing heat, and the vapor returns to a condenser (often water-cooled) where it condenses back to liquid. This approach reduces required mass flow and pumping power compared to single-phase liquid cooling and can significantly improve energy efficiency.

Figure 1. Conceptual R2L pumped two-phase cooling architecture (schematic)

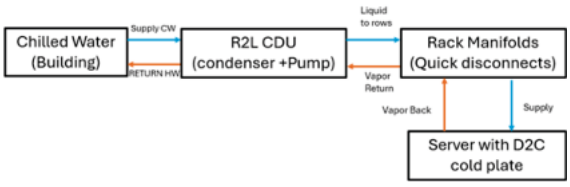

Figure 1. Conceptual R2L Pumped Two-phase Cooling Architecture (Schematic).

2. Experimental Setup

The cooling system consists of a central in-row Refrigerant-to-Liquid (R2L) Coolant Distribution Unit (CDU) with 160 kW nominal capacity, supplying refrigerant to multiple racks via quick-disconnect manifolds. The CDU contains a brine/water condenser (linked to the facility chilled water) and a high-pressure pump. Liquid refrigerant is sent to an overhead row manifold, which divides into rack-level manifolds ensuring equal flow. Each rack manifold branches via flexible hoses and quick-disconnects into four parallel cooling loops (CLs), each serving four micro-channel cold plates (CPs) mounted on heater cores inside a 3U Thermal Test Vehicle (TTV). Each TTV has a 2,500 mm² mounting area and a 2.5 kW cartridge heater; each CL thus absorbs up to 10 kW. A row of four racks (ten TTVs per rack) was assembled, giving a total test capacity of 160 kW. Flow to each CP array was controlled by fixed orifices/regulators (2–32 psi per loop). Returns converge through rack and row manifolds to the CDU condenser. Temperatures, pressures, and flow rates were monitored at the CDU, manifolds, and each loop inlet/outlet. R-134a was the primary refrigerant; compatible low-GWP alternatives (e.g., R-515B) were evaluated in parallel. Hydraulic tests varied pump flow from 20 to 36 LPM per rack (4.0–7.2 LPM per CL) at a constant supply temperature of 22 °C with no heat. Thermal tests incrementally increased heater power up to 10 kW per loop (40 kW per rack, 160 kW total).

Figure 2. Example pumped two-phase loop with two parallel evaporators and flow regulators (schematic).

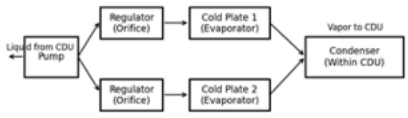

Figure 2. Example Pumped Two-phase Loop Schematic Showing Parallel Cold-plate Evaporators and Flow Regulators.

3. Governing Equations

Reynolds number (channel/mini-channel flow):

$$Re = \rho V D_h / \mu \quad (1)$$

For an array expressed via mass velocity G:

$$Re = G D_h / \mu \quad (2)$$

Nusselt number (definition):

$$Nu = h D_h / k \quad (3)$$

Effective chip-to-coolant thermal resistance (based on saturation temperature):

$$R_{th} = (T_{case} - T_{sat}) / Q \quad (4)$$

4. Results and Discussion

Hydraulic Performance. The row-level manifold showed very low pressure drop (<0.23 psi even at 36 LPM per rack), indicating efficient distribution. Rack manifolds, hoses, and cold-plate regulators dominated loop resistance: at 7.2 LPM per loop the loop ΔP reached ~7.6 psi, rising roughly quadratically with flow as expected. Fixed-orifice valves maintained a narrow pressure band (2–5 psi per loop) and balanced flow under uneven loads. Pumping power remained modest: for ~36 LPM total, the pump head was <35 psi to overcome all losses.

Thermal Performance. With all racks at 10 kW per loop, the refrigerant saturation temperature stabilized near 22–24 °C (depending on chilled-water inlet). Subcooling entering cold plates remained <5 °C at low loads, growing to ~15 °C at maximum load due to return-line pressure drop. At 0.48 LPM/kW, peak case temperature T_case plateaued at 56.4 °C

(40 kW per rack); at ~0.50 LPM/kW it dropped to ~55 °C, well below ~80 °C reliability limits. Loop-exit vapor quality stayed <0.60, avoiding dryout, and the effective cold-plate thermal resistance was ~0.012 °C/W at saturation.

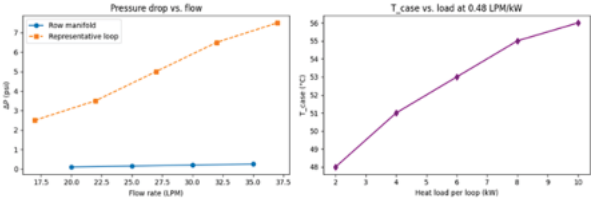

Figure 3. (Left) Measured pressure drops vs. flow for row manifold and representative rack loop. (Right) Heater case temperature vs. load at fixed flow (0.48 LPM/kW). Note: Where raw arrays were unavailable, synthetic points were constructed to match reported extrema and trends.

4.1 Pressure Drop Budget

At full load (40 kW/rack), total ΔP from CDU to loop exit was ~35 psi: ~0.23 psi across the row manifold; ~7.6 psi across the loop (hoses + regulators + CPs); and ~27 psi within the CDU condenser and internal piping. With pump capability near 40 psi, there is margin for higher flows or lower T_sat. The small distribution ΔP confirms non-limiting manifold design.

5. Water vs PG25% (Propylene Glycol 25%)

Using 25% propylene glycol (PG25%) in water increases viscosity and reduces thermal conductivity relative to pure water, elevating pressure drop and lowering heat transfer coefficients in single-phase regions. In this two-phase architecture, primary impacts arise in facility-side condensers and auxiliary water loops: PG25% will require slightly higher pump head and may reduce approach temperature by a few degrees compared with water, while offering freeze protection and corrosion inhibition.

6. Comparison: Air vs Single-Phase vs Two-Phase

Air cooling in high-density racks often forces large blower power and high approach temperatures, with cooling consuming 25–40% of facility energy. Single-phase liquid cooling reduces chip-to-coolant resistance but requires high volumetric flow (e.g., 10–15 LPM per 10 kW loop with small ΔT), driving significant pump work. Pumped two-phase D2C leverages latent heat to cut required mass flow to ~0.5 LPM/kW and minimize temperature rise, reducing pump energy by an order of magnitude and enabling very low partial PUE values when paired with efficient heat rejection.

7. Failure Scenario Analysis

Pump failure: With proper check valves and pressure cutouts, a sudden pump stop isolates loops; capillary inventory and regulators limit backflow. Restart recovers nominal pressure rapidly without compressor cycling in R2L CDUs.

Flow imbalance: Fixed-orifice regulators maintain loop ΔP (2–5 psi) and balanced flow even under asymmetric loads or hot-swaps; observed temperature excursions were <1 °C on adjacent loops during pulsed-power tests.

8. CONCLUSIONS

A prototype R2L pumped two-phase D2C system with a 160 kW CDU safely dissipated up to 160–170 kW while maintaining chip case temperatures below 57 °C at ~0.48–0.50 LPM/kW. Hydraulic losses were modest, implying low pumping power and easy scalability toward 200 kW CDUs. The architecture achieved high efficiency via vaporization-driven heat transport and demonstrated robustness under asymmetric loading. Low-GWP refrigerants (e.g., R-515B) are compatible, improving sustainability without fundamental redesign.

9. Nomenclature

A — Area (m^2)
CP — Cold plate
CDU — Coolant Distribution Unit
CL — Cooling loop
D_h — Hydraulic diameter (m)
G — Mass velocity ($kg \cdot m^{-2} \cdot s^{-1}$)
h — Convective heat transfer coefficient ($W \cdot m^{-2} \cdot K^{-1}$)
k — Thermal conductivity ($W \cdot m^{-1} \cdot K^{-1}$)
Nu — Nusselt number
PG25% — 25% propylene glycol in water (vol%)
Q — Heat load (W)
Re — Reynolds number
R_th — Thermal resistance ($K \cdot W^{-1}$)
T_case — Chip/heater case temperature (°C)
T_sat — Refrigerant saturation temperature (°C)
TTV — Thermal Test Vehicle
V — Mean velocity ($m \cdot s^{-1}$)
ΔP — Pressure drop (psi or Pa)
μ — Dynamic viscosity (Pa·s)
ρ — Density ($kg \cdot m^{-3}$)

Appendix A: Figures and Tables

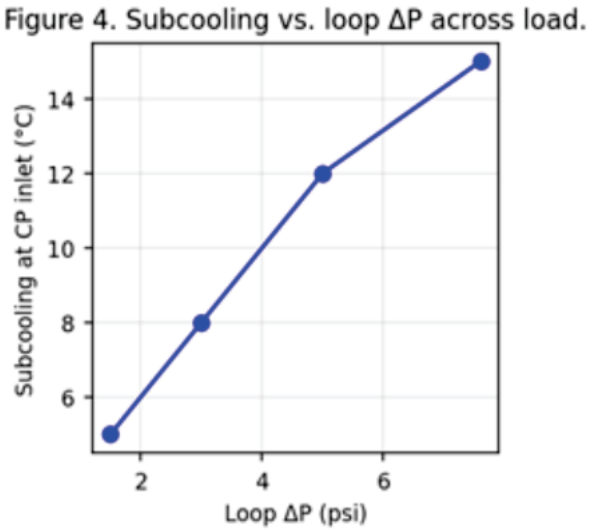

Figure 4. Subcooling vs. Loop Pressure Drop Across Load.

Table 1. Pressure Drop Budget at Full Load (40 kW/rack)

Component	ΔP (psi)	Notes
Row manifold	0.23	At 36 LPM per rack
Rack manifolds & hoses	0.8	Representative average across rack
Loop (regulators + CPs)	7.6	At 7.2 LPM per loop
CDU condenser & internal piping	27	From CDU gauges at full flow
Total (CDU to loop exit)	35	Full-load, full-flow condition

Table 2. Test Matrix

Rack/Loop	Flow (LPM)	Heat (kW)	T_sat (°C)	Subcooling (°C)
Rack A / Loop 1	4.8	6	23	6
Rack A / Loop 2	4.8	8	23	9
Rack B / Loop 1	6.0	10	24	12
Rack C / Loop 3	5.6	8	23	10
Rack D / Loop 4	7.2	10	24	15
Rack D / Loop 2	4.0	4	22	5

Table 3. Refrigerant Options and Key Properties

Refrigerant	Safety Class	GWP	Notes
R-134a	A1	1430	Benchmark HFC used in tests
R-515B (Solstice N15)	A1	299	Low-GWP azeotrope; similar pressures to R-134a

R-1234yf	A2L	~4	Ultra-low GWP HFO; mildly flammable

Appendix B: Worked Calculations

B.1 Flow Sizing (Two-phase Guideline)

Using the volumetric guideline for pumped two-phase direct-to-chip loops, $\dot{V} \approx 0.48–0.50$ LPM per kW. For a 10 kW loop: $\dot{V} = 0.48 \times 10 = 4.8$ LPM and $0.50 \times 10 = 5.0$ LPM.

B.2 Effective Thermal Resistance (R_th)

Definition: R_th = (T_case − T_sat) / Q

With T_case = 56.4 °C and T_sat = 23.0 °C: R_th,CP = (T_case − T_sat)/Q_CP = 33.4/2500 = 0.01336 K/W; R_th,loop = 33.4/10000 = 0.00334 K/W.

B.3 Row-manifold ΔP scaling vs. flow

Model: $\Delta P\_row(F) = 0.23 \times (F/36)\,\hat{}\,2$ [psi], based on $\Delta P\_row(36\ LPM) \approx 0.23$ psi.

Flow (LPM/rack)	ΔP_row (psi)
20	0.071
24	0.102
28	0.139
32	0.182
36	0.230

B.4 Loop ΔP reference points (measured)

Representative loop (hoses + regulators + CPs):

Loop flow (LPM/loop)	ΔP_loop (psi)
4.0	2.5
5.0	4.0
6.0	5.8
7.2	7.6

B.5 Reynolds and Nusselt (template)

Equations: $Re = (\rho V D_h)/\mu = (G D_h)/\mu$; $Nu = h D_h / k$. Inputs required per cold plate: hydraulic diameter D_h, channel count and flow area (to compute V or G), and refrigerant properties (ρ, μ, k) at the test pressure/temperature. To compute a sample h (boiling), select a validated two-phase correlation for mini/micro-channels (e.g., Kandlikar, Gungor–Winterton) with your channel geometry, mass flux, heat flux, and exit quality.

10. Acknowledgments

None.

11. REFERENCES

[1] Heydari, A., Al-Zu'bi, O., Manaserh, Y., Gharaibeh, A. R., Tipton, R., Mehrabikermani, M., Rodriguez, J., and Sammakia, B., 2025, 'Advancing in Data Centers Thermal Management: Experimental Assessment of Two-Phase Liquid Cooling Technology,' ASME J. Electron. Packag., 147(4), 041108. https://doi.org/10.1115/1.4069320. URL: asmedigitalcollection.asme.org/electronicpackaging/article/147/4/041108/1219979 (Accessed Feb 10, 2026).

[2] Heydari, A., Al-Zu'bi, O., Manaserh, Y., Gharaibeh, A. R., Tipton, R., Mehrabikermani, M., Rodriguez, J., and Sammakia, B., 2024, 'Advancing in Data Centers Thermal Management: Experimental Assessment of Two-Phase Liquid Cooling Technology,' Proceedings of InterPACK2024, San Jose, CA, Oct. 8–10, IPACK2024-141342. URL: par.nsf.gov/servlets/purl/10611032 (Accessed Feb 10, 2026).

[3] Vertiv, 2024–2026, 'Vertiv™ CoolPhase CDU,' Product Page and Documents. URL: www.vertiv.com/en-us/products-catalog/thermal-management/high-density-solutions/vertiv-coolphase-cdu/ (Accessed Feb 10, 2026).

[4] Vertiv, 2024, 'CoolPhase CDU Installer/User Guide (XDM300),' ManualsLib. URL: www.manualslib.com/manual/3642413/Vertiv-Coolphase-Cdu.html (Accessed Feb 10, 2026).

[5] Vertiv, 2025, 'Pumped two-phase direct-to-chip cooling: Advancing AI data center efficiency,' Blog, June 16. URL: www.vertiv.com/en-emea/about/news-and-insights/articles/blog-posts/pumped-two-phase-direct-to-chip-cooling-advancing-ai-data-center-efficiency/ (Accessed Feb 10, 2026).

[6] Advanced Cooling Technologies (ACT), 2025, 'ACT Unveils 200kW Two-Phase Liquid Cooling CDU,' News Release, Apr. 14. URL: www.1-act.com/about/news/200kw-two-phase-liquid-cooling-cdu/ (Accessed Feb 10, 2026).

[7] Advanced Cooling Technologies (ACT), 2024–2026, 'Pumped Two-Phase,' Application Page. URL: www.1-act.com/thermal-solutions/active/pumped-two-phase/ (Accessed Feb 10, 2026).

[8] Open Compute Project, 2025, 'Pumped 2P Refrigerant-Based Direct Liquid Cooling (DLC) Technology for Next Generation AI Clusters with High TDP Accelerators,' White Paper v1.0, Feb. 14. URL: www.opencompute.org/documents/2p-refrigerant-based-dlc-wp-v1-pdf-1 (Accessed Feb 10, 2026).

[9] ARPA-E, 2024–2026, 'COOLERCHIPS Program Overview,' U.S. DOE ARPA-E. URL: arpa-e.energy.gov/programs-and-initiatives/view-all-programs/coolerchips (Accessed Feb 10, 2026).

[10] IBM Research, 2023, 'Systems Two-Phase Cooling,' COOLERCHIPS Kickoff Presentation, Oct. 18–19. URL: arpa-e.energy.gov/sites/default/files/2025-06/Day1_06b_10-25-23%20IBM%20COOLERCHIPS%20Kick-off_SystemsTwoPhaseCooling_ForDistribution.pdf (Accessed Feb 10, 2026).

[11] Uptime Institute, 2021, 'Does the spread of direct liquid cooling make PUE less relevant?' Blog, Nov. 5. URL: journal.uptimeinstitute.com/does-the-spread-of-direct-liquid-cooling-make-pue-less-relevant/ (Accessed Feb 10, 2026).

[12] Honeywell, 2024–2026, 'Solstice® N15 (R-515B) Technical Data Sheet.' URL: prod-edam.honeywell.com/content/dam/honeywell-edam/pmt/oneam/en-us/refrigerants/documents/pmt-am-515b-tds.pdf (Accessed Feb 10, 2026).

[13] ASHRAE/UNEP, 2022, 'Update on New Refrigerants Designations and Safety Classifications,' Fact Sheet. URL: www.ashrae.org/file%20library/technical%20resources/bookstore/factsheet_ashrae_english_november2022.pdf (Accessed Feb 10, 2026).

[14] AHRI, 2011–2025, 'Low-GWP Alternative Refrigerants Evaluation Program (AREP),' Program Page and Reports. URL: www.ahrinet.org/analytics/research/ahri-low-gwp-alternative-refrigerants-evaluation-program (Accessed Feb 10, 2026).